Evaluation of Inkjet Printhead Materials Using EIS

James M. Mrvos; Lexmark International; Lexington, Kentucky/USA

Abstract

Electrochemical Impedance Spectroscopy (EIS) was used to assess the ability of two different epoxy die attach adhesives to prevent corrosion of copper. Incorporating corrosion inhibitors in the adhesives was shown to reduce but not eliminate corrosion. EIS revealed that high water absorption in adhesives with low crosslink density significantly increased corrosion. Chloride impurities in the adhesives also increased corrosion. The diffusion coefficient of chloride in the epoxy was found to be 5 to 6 orders of magnitude lower than water. The presence of two time constants in the EIS scans correlated well with more corrosion.

Introduction

Corrosion is an incessant problem in inkjet printheads, where fluids and metals contact each other while electrical bias is applied. Printhead encapsulants, covercoats, photoresists, and die attach adhesives are extensively tested to verify their ability to prevent corrosion of heater chips and interconnect circuits. Large numbers of assemblies are tested for many weeks to ensure that the material set and the manufacturing process provide protection from corrosion. As the service life requirement of inkjet printheads increases, prevention of corrosion becomes a major challenge and the cost and time needed for testing increases. Electrochemical impedance spectroscopy (EIS) is a powerful technique used for assessing the corrosion resistance provided by organic coatings on metals [1][2] and the effectiveness of corrosion inhibitors [3]. A two week EIS test can determine the ability of printhead materials to protect against corrosion. Using traditional methods, this same information takes months to obtain.

Theory

Corrosion of a metal is an electrochemical process in which the material is oxidized by the exchange of electrons with the surrounding environment. The corrosion process therefore, causes electrical potentials and currents to be generated.

When a specimen of a metal coated with a polymer is immersed in an electrolyte solution and a sinusoidal electrical potential is applied, the current response will behave like a circuit containing parallel resistors and capacitors. By applying Euler's theorem, the impedance of this system can be expressed as a complex number using Ohm's law for AC circuits [1]:

$$Z = \frac{E}{I} = |Z|\frac{\sin(\omega t)}{\sin(\omega t + \theta)} = |Z|(\cos\theta + j\sin\theta) \qquad (1)$$

where Z = impedance of the system, E = applied potential, I = current, |Z| = magnitude of the impedance, ω = angular frequency of the potential, θ = phase angle, t = time, and $j = (-1)^{1/2}$. It is evident from Equation 1 that impedance varies with frequency and that there will be a lag in the current response to changes in the potential equal to the phase angle. As will be demonstrated, resolving the impedance into real and imaginary components provides a useful means to analyze the results of EIS experiments.

The impedance of a resistive circuit element, Z′, is a real number that is equal to its resistance, R. However, the impedance of capacitive circuit element, Z″, is an imaginary number inversely proportional to its capacitance, C:

$$Z' = R = |Z|\cos\theta, \qquad Z'' = \frac{1}{j\omega C} = \frac{-j}{\omega C} = |Z|j\sin\theta \qquad (2)$$

As suggested by Equation 1, the total impedance at any frequency is calculated by adding Z′ and Z″. The magnitude of the impedance is related to Z′ and Z″ by the equation:

$$|Z| = \sqrt{(Z')^2 + (Z'')^2} \qquad (3)$$

In EIS studies, equivalent circuits composed of resistors, capacitors, and other passive elements are used to model the physical and mathematical behavior of electrochemical systems. Impedances for parallel and series components of a system are combined using the same rules used in DC electronics: series impedances are summed and the reciprocals of parallel impedances are summed.

The circuit shown in Figure 1 is frequently used to model a corroding metal coated with a polymer that is exposed to a solution containing an electrolyte [4]. For an inkjet printhead, this system corresponds to ink in contact with a metal electrical trace on a circuit. The trace is protected from contact with ink by an encapsulating polymeric adhesive. In the model, R_s is the resistance of the ink, C_{coat} is the coating capacitance (charge flowing through an interface creates a capacitance), and R_{pore} is the pore resistance of the coating. C_{dl} is the capacitance of the double layer formed at the metal/ink interface as the coating delaminates. R_{ct} is the charge transfer resistance that develops as electrons are transferred between the metal and the ink. R_{ct} is also known as the polarization resistance. The corrosion rate of a metal will be inversely proportional to R_{ct} [4]. W represents a Warburg diffusion element (discussed below).

In an EIS experiment, a low amplitude AC signal is applied to an electrochemical test cell. The frequency of the signal is ramped from a high frequency to a low frequency. Using Equation 1, |Z| and θ are calculated at each frequency based on the applied potential and the current response. Z′ and Z″ are then calculated using Equation 2. Impedance data are often represented in a graph of -Z″ versus Z′ called a Nyquist plot.

Figure 2 is a Nyquist plot for the circuit shown in Figure 1 using typical values for the resistances and capacitances. It should be noted that frequency is not explicitly shown in a Nyquist plot. High frequency data are plotted near the origin and low frequency data are at the right of the graph.

The 45° line on the right side of Figure 2 indicates that a Warburg diffusion element is present. The Warburg coefficient, σ, can be found from the slope of a plot of Z′ versus $\omega^{-1/2}$ [2]. The diffusion coefficient of the electrolyte in the coating can be estimated from the Warburg coefficient using the equation [5]:

$$\sigma = \left(\frac{RT}{(nF)^2}\right)\left(\frac{1}{\sqrt{2}}\right)\left(\frac{1}{c\sqrt{D}}\right) \quad (4)$$

where R = gas constant, T = absolute temperature, n = number of electrons transferred in the reaction, F = Faraday constant, c = electrolyte concentration, and D = diffusion coefficient.

In Figure 3, the same set of data is plotted in the Bode format which reveals the relationship of |Z| and θ versus frequency. Using Equation 2, C_{coat} can be calculated from the slope of the linear portion of the Bode |Z| plot in the high frequency region. When a metal specimen with a polymer coating is initially placed in a solution, the R_{pore} is usually very high. This causes all the current to flow through C_{coat}. The Nyquist plot will be a vertical line and very little information can be obtained from it. However, the C_{coat} value found from the Bode |Z| plot can be used to calculate the dielectric constant of the specimen [6]:

$$C_{coat} = \frac{\varepsilon_o \varepsilon A}{d} \quad (5)$$

where ε = dielectric constant, ε_o = permittivity of free space (8.85×10^{-14}F/cm), A = contact area, and d = coating thickness. Coatings with high dielectric constants will provide better electrical insulation. As water is absorbed into a coating, its capacitance will increase because the dielectric constant of water (80) is about 20 times higher than the dielectric constant of a typical organic coating [2]. Capacitance data can also be used to provide a means of determining a coating's water uptake [6]:

$$V(t) = \log\left(\frac{C(t)}{C_0}\right) \Big/ \log(80) \quad (6)$$

where V(t) and C(t) are the volume fraction of water and the C_{coat} value measured at time t. C_0 is the initial coating capacitance.

The Bode phase angle plot shows another important characteristic of the electrochemical system under study. The two local maxima in Figure 3 at about 600 Hz and 60 kHz indicate that the system has two RC time constants. This two time constant behavior manifests itself in the Nyquist plot as a partially resolved semicircle in the high frequency region associated with C_{coat} and R_{pore}. The fully resolved semicircle on the right is associated with C_{dl} and R_{ct}. When there is only one time constant, the C_{dl} and R_{ct} elements are ignored and the circuit used to model the system contains only R_s, C_{coat} and R_{pore}. This is known as a Randles cell.

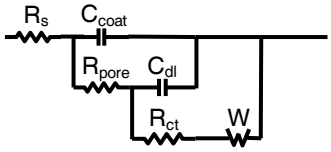

Figure 1. *Equivalent Circuit Representation*

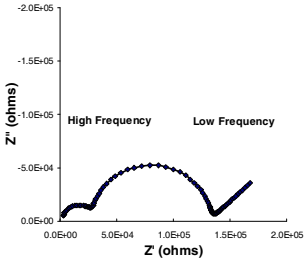

Figure 2. *Example of Nyquist plot*

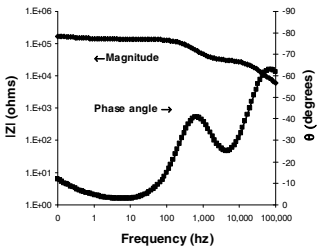

Figure 3. *Example of Bode Plot*

Experimental

The design of the experiment is shown in Table 1. Two epoxy die attach adhesives were evaluated. The primary difference between the adhesives was the crosslink density. Adhesive 1 had a greater crosslink density and hence a higher modulus than Adhesive 2 (450 MPa vs. 1 MPa). Both adhesives contained a chloride contaminant due to impurities in the raw materials. The chloride content was <50 ppm for Adhesive 1 and >1000 ppm for Adhesive 2. Two different inorganic corrosion inhibitors (A and B) and two different liquids (an aqueous solution of 15 ppm of chloride as NaCl and de-ionized water) were included in the experiment. The conductivities of the DI water and the 15 ppm chloride solution were 1 μSiemen and 29 μSiemen, respectively. DI water was chosen because it would not contribute ions to the system. Therefore it would provide a better assessment of the adhesive's tendency to cause corrosion due to impurities in its formulation. The 15 ppm Cl solution was used in order to mimic the anion content of the ink. The thickness of each adhesive specimen was measured prior to the start of the experiment using a micrometer so that dielectric constant calculations could be performed. Throughout the experiment, the cells were kept in a 60°C oven. EIS scans were made at time 0 and then once per day.

The specimens were mounted in Princeton Applied Research Model K0235 electrochemical flat cells equipped with Ag/AgCl reference electrodes. Figure 4 is a diagram of the cell. The choice of Ag/AgCl was made in order to provide thermal stability at the 60°C test temperature. Specimens were prepared by coating and curing a ~500 μm thick layer of adhesive onto a 25 μm layer of copper that was deposited on 50 μm thick polyimide film. A luggin capillary was used to provide a means for measuring the potential within approximately 1 mm of the specimen's surface. The specimen was clamped to the end of the flat cell so that it contacted the solution through a 1 cm^2 opening in the cell.

The cells were connected to a Princeton Applied Research Model 273A potentiostat, a Solartron Model 1255B frequency response analyzer, and a Solartron Model 1281B multiplexer. The instrumentation was controlled using Scribner Associates Inc. CorrWare v. 2.9c electrochemical software and ZPlot v. 2.9c EIS software. Scribner ZView v. 2.9c was used to calculate capacitances and resistances by complex number least squares (CNLS) fitting.

EIS scans were made by sweeping the frequency from 100 kHz to 0.1 Hz using 10 steps per decade. The amplitude of the signal was 100 mV. EIS scans are typically made at 10 mV for coatings less than 25 μm thick. The higher amplitude was chosen in order to improve the response of the 500 μm coating. A bias of +4 V versus the open circuit potential was applied during the scan to mimic the bias on the heater chip during its operation.

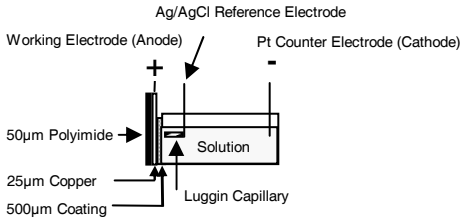

Figure 4*. Flat Cell Configuration*

Adhesive	Additive	Solvent
1	None	DI
1	A	DI
1	B	DI
1	None	DI/15ppm Cl
1	A	DI/15ppm Cl
1	B	DI/15ppm Cl
2	None	DI
2	B	DI
2	None	DI/15ppm Cl
2	B	DI/15ppm Cl

Table 1. *Experimental Design*

Results and Discussion

Figures 5A-D are plots of C_{coat} and R_{pore} calculated for each scan. Table 2 shows the dielectric constants, the water volume fractions in the coatings after 1 day, and the average values for R_{ct} and C_{dl} for the days when two time constants were present in the scans. Table 2 also includes a visual ranking for each of the specimens at the end of the experiment. Pitting corrosion and surface oxidation was present on all the specimens. Three of the six Adhesive 1 specimens and 3 of the four Adhesive 2 specimens exhibited two time constants during at least part of the experiment.

In Figure 5A, the capacitance data for all the Adhesive 1 combinations follow the same trends. Initial values of C_{coat} were in the range of $4x10^{-11}$ F to $1x10^{-10}$ F. A peak in the C_{coat} value occurred after 1 day followed by a slight reduction in subsequent days. All of the C_{coat} values settled in the range of $1.3x10^{-10}$ F to $2.2x10^{-10}$ F. The increase of C_{coat} was due to an increase in the water content of the coating. The slight reduction in C_{coat} at longer exposure times occurred because of swelling. The Additive B/15 ppm Cl specimen exhibited the greatest increase in C_{coat} during the early stages of the experiment. It is likely that this material absorbed more water than the other Adhesive 1 specimens.

Figure 5B shows that R_{pore} of Adhesive 1 changed much more dramatically than C_{coat}. At time 0, all the specimens had very high R_{pore} values (greater than 10^{14} Ω). The R_{pore} values for all of the Adhesive 1 samples dropped 8-9 orders of magnitude within a few days to $2x10^{5}$ Ω – $8x10^{6}$ Ω. This behavior was due to the filling of the pores in the coating with water, providing a conductive path to the underlying metal.

As shown in Table 2, C_{dl} for Adhesive 1/No Additive/DI was $6.6x10^{-10}$ F. For Adhesive 1/No Additive/Cl, C_{dl} was $4.3x10^{-9}$ F. The C_{dl} value for Adhesive 1/Additive B/Cl was $1.6x10^{-7}$ F. From DC electronics, it is known that capacitance is inversely proportional to charge separation. Thus a higher C_{dl} value indicates the electrical double layer thickness has decreased. As ionic content at an interface increases, the double layer thickness decreases. Therefore, there must be a higher ionic content at the copper interface for the Cl samples compared to the DI specimen.

Figure 5C shows that the initial values of C_{coat} for Adhesive 2 were about half an order of magnitude higher than those for Adhesive 1. Furthermore, C_{coat} stayed relatively constant during the experiment, holding in the range of $1x10^{-10}$ F to $3x10^{-10}$ F. Evidently, Adhesive 2 absorbed a considerable amount of water within minutes of being exposed. This is consistent with the low crosslink density of the material.

As shown in Figure 5D, the shapes of the R_{pore} curves for Adhesive 2 were very similar to Adhesive 1. However, the initial values of R_{pore} were significantly lower, ranging between $3.3x10^{6}$ Ω to$1.5x10^{8}$ Ω compared to greater than 10^{14} Ω for Adhesive 1. This supports the conclusion that water was being rapidly absorbed by Adhesive 2. The steady state values of R_{pore} were between $3.3x10^{4}$ Ω and $1.3x10^{5}$ Ω – well over an order of magnitude lower than the majority of the Adhesive 1 R_{pore} values.

The same additive/solution combinations that showed two time constants with Adhesive 1 showed two time constants for Adhesive 2. The values of R_{ct} for Adhesive 2 were over an order of magnitude lower than for Adhesive 1. This indicates that the corrosion rate for the Adhesive 2 specimens was 10 times the rate for Adhesive 1.

Dielectric constants were calculated using Equation 5 and the volume fractions of water in the coatings after 1 day were calculated using Equation 6. These results are compiled in Table 2. For Adhesive 1 in either DI or 15 ppm Cl, ε followed the trend of Additive B<Additive A<No Additive. Because the capacitance and dielectric constant both increase as water content increases, it is apparent that Additive B initially resisted water absorption. However, the calculation of water volume fraction after 1 day reveals that this characteristic rapidly disappeared. The dielectric constants calculated for Adhesive 2 are all unreasonably high, due to the high initial capacitances. This confirms that was rapid absorption of water by this coating during the initial measurement caused by low crosslink density. The water volume fraction calculations for Adhesive 2 are not valid because they depend on the initial capacitance value when little or no water has been absorbed. Since water absorbed so rapidly, an accurate initial capacitance calculation could not be made.

Warburg diffusion elements were observed in only 3 of the scans: Adhesive 1/Additive B/Cl/4 day, Adhesive 2/No Additive/Cl/4 day, and Adhesive 2/Additive B/Cl/4 day. The diffusion coefficients for Cl in the adhesives calculated using Equation 4 were in the range of 10^{-17} to 10^{-18} m^2/cm. These are 5 to 6 orders of magnitude lower than the value of the water diffusion coefficient in epoxies determined by Fick's law. The low value of the diffusion coefficient is consistent with results from DSIMS experiments that found the diffusion coefficient of Cl in an epoxy was nine orders of magnitude lower than water [7]. The lack of Warburg elements in most of the scans indicates that the corrosion of the metal is not mass transfer limited by the diffusion of Cl from the solution to the surface. Also, since there was corrosion on the DI specimens, it can be concluded that the Cl impurity in the adhesives was able sustain the kinetically limited reaction. Moreover, the generally worse behavior of specimens in the 15 ppm Cl solution indicates that even very small levels from the slow diffusion of Cl to the metal interface increases corrosion.

Visual assessment of the Adhesive 1 specimens revealed that in DI, Additive A was more effective in preventing corrosion than Additive B. Additive B was ineffective in Cl. Two of the poorest performing specimens were the no additive samples in DI and in 15 ppm Cl. The 3 worst Adhesive 1 specimens all exhibited two time constant behavior during the test. The corrosion in Cl was usually more extensive than the same Adhesive/Additive combination in DI. As would be expected given the low values of R_{pore}, the levels of corrosion for Adhesive 2 were noticeably higher than for Adhesive 1. Additive B provided very limited protection against corrosion. The high water uptake and high level of Cl impurity could not be overcome by the additive. As with

Adhesive 1, two time constants for Adhesive 2 indicated poor corrosion performance.

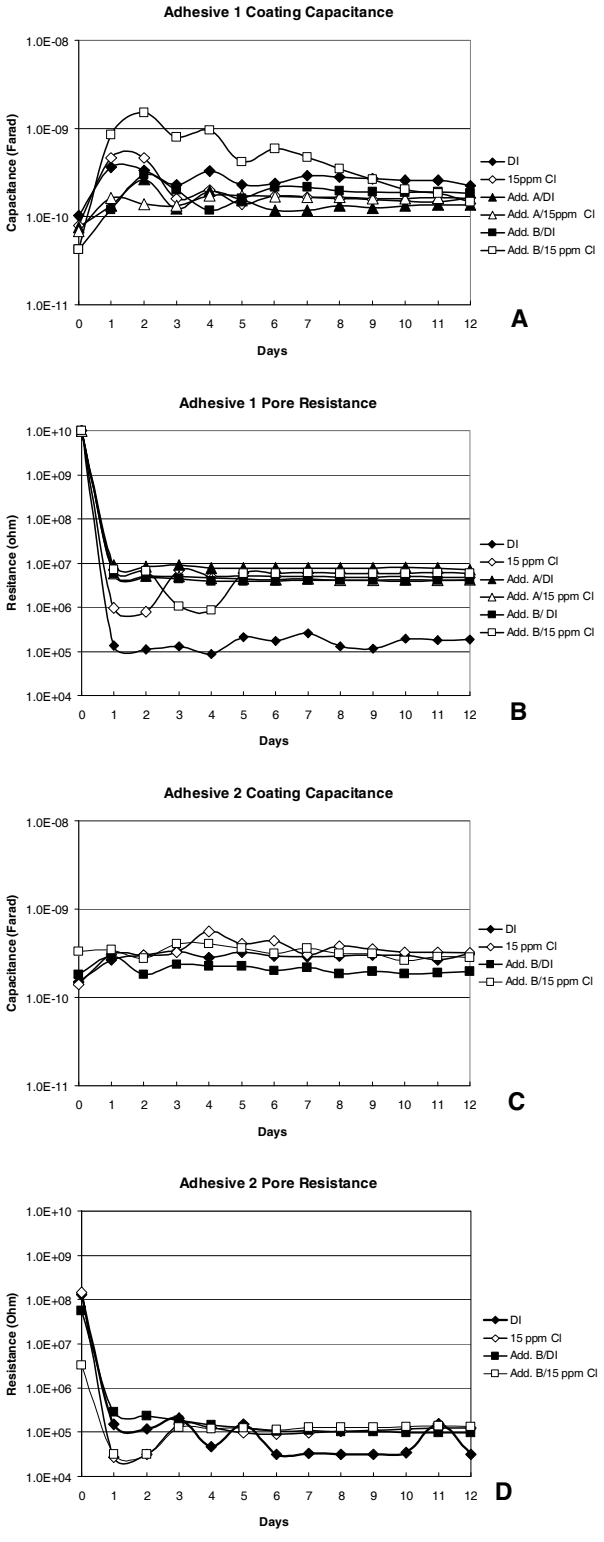

***Figure 5**. Experimental Results. **A:** Adhesive 1 C_{coat}, **B:** Adhesive 1 R_{pore}, **C:** Adhesive 2 C_{coat}, **D**: Adhesive 2 R_{pore}*

Adhesive	Additive	Solvent	ε	V	R_{ct} (ohm)	C_{dl} (F)	Days 2 RC Present	Rank
1	None	DI	56	0.13	3.4E+06	6.6E-10	1-2	4
1	A	DI	52	0.13	-	-	-	1
1	B	DI	33	0.24	-	-	-	2
1	None	15ppm Cl	67	N/A	5.6E+06	4.3E-09	1-2	5
1	A	15ppm Cl	44	N/A	-	-	-	3
1	B	15ppm Cl	26	N/A	4.8E+06	1.6E-07	3-4	6
2	None	DI	107	0.13	1.6E+05	9.5E-09	1-2,4,6-10,12	1
2	B	DI	111	0.11	-	-	-	2
2	None	15ppm Cl	87	N/A	9.3E+04	1.4E-09	1-2	4
2	B	15ppm Cl	229	N/A	1.1E+05	1.3E-09	1-2	3

***Table 2.** Dielectric Constant (ε), Water volume fraction after 1 day (V), Average charge transfer resistance (R_{ct}), Average double layer capacitance (C_{dl}), Days two RC constants were observed, Adhesive group rank (1=best)*

Conclusions

EIS has been shown to be a useful tool for assessing the ability of an adhesive to protect a metal from corrosion. Scans of the adhesives demonstrated that water absorption was the primary driving force for corrosion. Lower crosslink density caused higher water absorption and more corrosion. Chloride impurities in the adhesives also increased corrosion. Exposure to 15 ppm chloride/DI generated more corrosion than DI water alone. Incorporating corrosion inhibitors in the adhesive formulations reduced the extent of the corrosion. The presence of two RC time constants in the EIS scan during the course of the experiment correlated well to higher levels of corrosion.

In addition to testing die attach adhesives, EIS has successfully been used to provide insight into ability of interconnect circuit covercoat materials, electronic package encapsulants and negative photoresists used for heater chip passivation to prevent corrosion.

Acknowledgements

Thanks to Dr. Steven Yu, Mr. David Graham Ms. Qing Zhang, Mr. Samuel Sexton, Mr. Dale Rodgers, Ms. Karen Cui, Dr. Dell Rosa, Dr. Jianhua Su, Mr. James Vana, and Dr. Jack Morris.

References

[1] E. Barsoukov, J.R. MacDonald eds., Impedance Spectroscopy Theory, Experiment, and Applications (Wiley Interscience, Hoboken, NJ, 2005).
[2] J.R. Scully, D.C. Silverman, M.W. Kendig eds., Electrochemical Impedance: Analysis and Interpretation (ASTM, Philadelphia, PA, 1993).
[3] F. Gui, R.G. Kelly, Electrochemica Acta, 51, 1797 (2006).
[4] D. Loveday, et. al, JCT Coatings Tech, 88 (October 2004).
[5] S.R. Taylor, E. Gileadi, Corrosion, 51, 664 (1995).
[6] B.M. Brasher, A.H. Kingsbury, J. Appl. Chem., 4, 62 (1954).
[7] L. Lantz, M.G. Pecht, A Comparison of Ion Diffusion and Moisture Diffusion in a Commercial Epoxy Molding Compound, 2003 International Symposium on Microelectronics, pg. 477 (2003).

Author Biography

James Mrvos, PE, received his BS in chemical engineering from Carnegie Mellon University (1981) and his MS in chemical engineering from the University of Kentucky (1991). He has twenty-seven years of experience with Lexmark International and IBM in the manufacture and development of imaging supplies. Mr. Mrvos is a Lexmark senior technical staff member focusing on inkjet printhead process and materials research. Jim is the co-author of 43 issued and pending U.S. patents.